

# Nonlinear translational symmetric equilibria relevant to the L-H transition

Ap Kuiroukidis\* and G. N. Throumoulopoulos<sup>†‡</sup>

November 28, 2017

## Abstract

Nonlinear  $z$ -independent solutions to a generalized Grad-Shafranov equation (GSE) with up to quartic flux terms in the free functions and incompressible plasma flow non parallel to the magnetic field are constructed quasi-analytically. Through an ansatz the GSE is transformed to a set of three ordinary differential equations and a constraint for three functions of the coordinate  $x$ , in cartesian coordinates  $(x, y)$ , which then are solved numerically. Equilibrium configurations for certain values of the integration constants are displayed. Examination of their characteristics in connection with the impact of nonlinearity and sheared flow indicates that these equilibria are consistent with the L-H transition phenomenology. For flows parallel to the magnetic field one equilibrium corresponding to the H-state is potentially stable in the sense that a sufficient condition for linear stability is satisfied in an appreciable part of the plasma while another solution corresponding to the L-state does not satisfy the condition. The results indicate that the sheared flow in conjunction with the equilibrium nonlinearity play a stabilizing role.

---

\*Technological Education Institute of Serres, 62124 Serres, Greece

<sup>†</sup>University of Ioannina, Association Euratom-Hellenic Republic, Department of Physics, GR 451 10 Ioannina, Greece

<sup>‡</sup>E-mails: kourouki@astro.auth.gr, gthroum@uoi.gr

# 1 Introduction

For axisymmetric toroidal plasma equilibria the force-balance equation and Maxwell's equations reduce to the Grad-Shafranov equation (GSE) for the poloidal magnetic flux function  $\psi$  [1], [2]. Analytical solutions to the GSE are obtained by specifying the plasma pressure and poloidal current functions of  $\psi$ , usually in such a way as to linearize the resulting partial differential equation, e.g. [3]-[12]. Analytical solutions to the GSE are very useful for theoretical studies of plasma equilibrium, transport and stability as well as benchmarks for numerical codes [13]. Also it has been established in a variety of magnetic configurations that sheared flows can reduce turbulence and produce transport barriers, which under certain conditions can extend to the whole plasma, e.g. [14]. In view of a fusion reactor the spontaneous formation of transport barriers, i.e., those driven by internal processes even in the absence of external sources, is of particular interest. For this reason among others stationary equilibria with plasma flow have been extensively studied on the basis of generalized GSEs, e.g. [15]-[37]. In particular, although complex numerical codes are extensively used to attempt simulations of the L-H transition, certain equilibrium considerations in connection with this transition are helpful, e.g. [38]-[41].

The simplest known and widely used in various studies, analytical solution to the GSE, is the Solovév equilibrium [3]. Extension of the original Solovév solution, to include the possibility of sheared flows appeared in [23]. In other extensions additional free parameters were introduced to construct configurations with fusion relevant plasma boundaries and desirable values of confinement figures of merit as the safety factor on magnetic axis [11, 12, 34]. Most of the solutions are associated with pressure and current profiles, including up to quadratic terms in the flux function  $\psi$  to linearize the resulting equation [3]-[12]. Linear equilibria with flow were constructed in [15]-[35] and in Refs. cited therein. Also, the non linear translational symmetric equilibria of “cat eyes” and counter rotating vortices with flow parallel to the magnetic field were studied in [36, 37]. These nonlinear equilibria, however, are periodic in one direction ( $x$ ) and therefore the plasma is not bounded along this direction.

In most of the above cases the axisymmetric equilibria are obtained as separable solutions of GSE. A novel non-separable class of solutions was found in Ref. [30] describing up-down symmetric configurations with incompressible flows parallel to the magnetic field and it was extended recently to

include asymmetric configurations [31] and flows of arbitrary direction [35]. For non parallel flows the question of the stability is usually not considered and this is partly due to the difficulty of the subject and the absence of a concise criterion. Few sufficient conditions for linear stability are available only for parallel flows [42]-[44]. In previous studies we found that the stability condition of Ref. [44] is not satisfied for the linear equilibria of [27] and [34] while it is satisfied within an appreciable part of the plasma for the nonlinear equilibria of [36] and [37]. This led us to the conjecture that the equilibrium nonlinearity may act synergetically with the sheared flow to stabilize the plasma.

Aim of the present study is to construct certain two dimensional non-linear up-down symmetric equilibria with incompressible flow of arbitrary direction in  $z$ -independent geometry. They are more pertinent to a magnetically confined plasma than those of Refs. [36] and [37] because the plasma is bounded on the poloidal plane. Another reason for considering translational symmetry is the many free physical and geometrical parameters involved in connection with the flow amplitude, direction and shear, equilibrium nonlinearity, symmetry and toroidicity. Thus, in the presence of nonlinearity one first could exclude toroidicity. The study is performed quasi-analytically through a non separable ansatz under which the GSE is transformed to a set of three ordinary differential equations and a constraint for three functions. The solutions give nested magnetic surfaces and their characteristics are studied by means of certain equilibrium quantities and confinement figures of merit as the safety factor, electric field and  $\mathbf{E} \times \mathbf{B}$  velocity shear. Also, for parallel flows the linear stability is considered by means of the aforementioned sufficient condition [44]. The results are in qualitative agreement with phenomenological characteristics of an edge transport barrier, confirm relevant scenarios [14], [23] and support the above conjecture.

The organization of the paper is as follows: In the first section we briefly review the general setting for the equations of incompressible flow with translational symmetry together with the generalized GSE. In Section II the proposed ansatz and the resulting equations are presented which then are integrated numerically. In section III we consider the solutions for certain values of the various parameters and integration constants and discuss the most important equilibrium properties. In section IV the criterion for linear stability is applied to the equilibria constructed for parallel flows. Section V summarizes the study and briefly proposes potential extensions.

## 2 Translational Symmetric Equilibria with flow

The equilibrium of a cylindrical plasma with incompressible flow and arbitrary cross-sectional shape, satisfies [19], [23],

$$(1 - M_p^2)\nabla^2\psi - \frac{1}{2}(M_p^2)'|\nabla\psi|^2 + \frac{d}{d\psi}\left(\mu_0 P_s + \frac{B_z^2}{2}\right) = 0 \quad (1)$$

for the poloidal magnetic flux function  $\psi$ . Here,  $M_p(\psi)$ ,  $P_s(\psi)$ ,  $\rho(\psi)$  and  $B_z(\psi)$  are respectively the poloidal Alfvén Mach function, pressure in the absence of flow, density and magnetic field parallel to the symmetry axis  $z$ , which are surface quantities. Because of the symmetry, the equilibrium quantities are  $z$ -independent and the axial velocity  $v_z$  does not appear explicitly in (1). Derivation of (1) is based on the following two steps: First, express the divergence free fields in terms of scalar quantities as

$$\begin{aligned} \mathbf{B} &= B_z\nabla z + \nabla z \times \nabla\psi \\ \mu_0\mathbf{j} &= \nabla^2\psi\nabla z - \nabla z \times \nabla B_z \\ \rho\mathbf{v} &= \rho v_z\nabla z + \nabla z \times \nabla F \end{aligned}$$

and the electric field by  $\mathbf{E} = -\nabla\Phi$ . Second, project the momentum equation,  $\rho(\mathbf{v} \cdot \nabla)\mathbf{v} = \mathbf{j} \times \mathbf{B} - \nabla P$ , and Ohm's law,  $\mathbf{E} + \mathbf{v} \times \mathbf{B} = 0$ , along the symmetry direction  $z$ ,  $\mathbf{B}$  and  $\nabla\psi$ . The projections yield four first integrals in the form of surface quantities (two out of which are  $F(\psi)$  and  $\Phi(\psi)$ ), Eq. (1) and the Bernoulli relation for the pressure

$$P = P_s(\psi) - \frac{1}{2\mu_0}M_p^2(\psi)|\nabla\psi|^2 \quad (2)$$

Because of the flow  $P$  is not a surface quantity. Also the density becomes surface quantity because of incompressibility and  $M_p^2(\psi) = (F'(\psi))^2/(\mu_0\rho)$ . Five of the surface quantities, chosen here to be  $P_s$ ,  $\rho$ ,  $B_z$ ,  $M_p^2$  and  $v_z$ , remain arbitrary.

Using the transformation

$$u(\psi) = \int_0^\psi [1 - M_p^2(g)]^{1/2} dg, \quad (M_p^2 < 1) \quad (3)$$

Eq. (1) is transformed to

$$\nabla^2 u + \frac{d}{du} \left( \mu_0 P_s + \frac{B_z^2}{2} \right) = 0 \quad (4)$$

Note that transformation (3) does not affect the magnetic surfaces, it just re-labels them. Eq. (4) is identical in form with the static equilibrium equation. In the present study we assign the free function term in (4) as

$$\left( \mu_0 P_s + \frac{B_z^2}{2} \right) = c_0 + c_1 u + c_2 \frac{u^2}{2} + c_3 \frac{u^3}{3} + c_4 \frac{u^4}{4} \quad (5)$$

where  $c_0, c_1, \dots, c_4$  are free parameters.

### 3 Proposed Ansatz

We use Eq. (5) into Eq. (4), employ the ansatz

$$u = \frac{N_1(x)y^2 + f(x)D_0(x)}{y^2 + D_0(x)} \quad (6)$$

and equate the nominator of the resulting equation to zero. From the  $y^6$ -terms we obtain (a prime denotes derivative with respect to  $x$ )

$$N_1'' + c_1 + c_2 N_1 + c_3 N_1^2 + c_4 N_1^3 = 0 \quad (7)$$

From the  $y^0$ -terms we obtain the constraint  $C_s = 0$ , where

$$C_s = 2(N_1 - f) + D_0[c_1 + c_2 f + c_3 f^2 + c_4 f^3] = 0 \quad (8)$$

The  $y^4$  and  $y^2$ -terms, after rearrangement yield

$$f'' + 2(N_1 - f) \left( \frac{D_0'}{D_0} \right)^2 - \frac{8(N_1 - f)}{D_0} + c_4(N_1 - f)^3 = 0 \quad (9)$$

and

$$\begin{aligned} D_0'' + 2 \frac{(N_1' - f')}{(N_1 - f)} D_0' + 2 \frac{(D_0')^2}{D_0} - 6 + \\ + c_3 D_0 (N_1 - f) + 3c_4 D_0 N_1 (N_1 - f) = 0 \end{aligned} \quad (10)$$

Eq. (7) is solved using the tanh method [45], a method of solving non linear differential equations, which also employed in [29]. We have two solutions. The first is  $N_1(x) = a_0 + a_1 \tanh(vx)$ , where

$$\begin{aligned}
c_1 + c_2 a_0 + c_3 a_0^2 + c_4 a_0^3 &= 0 \\
c_2 + c_3(2a_0) + c_4(3a_0^2) &= 2v^2 \\
c_3 + c_4(3a_0) &= 0 \\
c_4(a_1^2) &= -2v^2
\end{aligned} \tag{11}$$

and the second is  $N_1(x) = a_0 + a_1 / \cosh(vx)$ , where

$$\begin{aligned}
c_1 + c_2 a_0 + c_3 a_0^2 + c_4 a_0^3 &= 0 \\
c_2 + c_3(2a_0) + c_4(3a_0^2) &= -v^2 \\
c_3 + c_4(3a_0) &= 0 \\
c_4(a_1^2) &= 2v^2
\end{aligned} \tag{12}$$

## 4 Solutions and equilibrium properties

We have solved numerically Eqs. (8), (9) and (10). Using the first of the solutions for  $N_1$ , namely the tanh solution, we obtained the equilibrium of Fig. 1. We have used  $a_0 = 1.1$ ,  $a_1 = 2.5$ ,  $v = 0.6$  and in Eq. (5)  $c_0 = 2.588$ ,  $c_1 = -0.638$ ,  $c_2 = 0.302$ ,  $c_3 = 0.38$ ,  $c_4 = -0.115$ . The boundary flux surface corresponds to  $u_b = 0.11$  while on the magnetic axis  $u_a = 0$ . The constraint was kept close to zero for the whole of the integration process and we got an average value of  $|C_s|$  equal to 0.10. Given the nonlinearity and complexity of the method this implies that the solution is indeed acceptable. Simple quadratic fitting gives

$$f = 1.272x^2 + 0.049x + 0.001 \text{ and } D_0 = 1.488x + 3.3.$$

Using the second of the solutions for  $N_1$ , namely the cosh solution, we obtained the equilibrium of Fig. 2. We have used  $a_0 = 1.0$ ,  $a_1 = -1.6$ ,  $v = 1.15$  and in Eq. (5)  $c_0 = 2.588$ ,  $c_1 = 0.289$ ,  $c_2 = 1.777$ ,  $c_3 = -3.099$ ,  $c_4 = 1.033$ . The boundary flux surface corresponds to  $u_b = -0.05$  while on the magnetic axis  $u_a = 0$ . The constraint was kept close to zero for the whole of the integration process and the average value of  $|C_s|$  was 0.01. Simple quadratic fitting gives  $f = -0.542x^2 + 0.009x$  and  $D_0 = 0.994x^2 + 3.3$ .

Here instead of the velocity  $v_z$  we have used the axial Mach function,  $M_z^2(u) = v_z^2/(B_z^2/(\mu_0\rho))$ , and the approximation  $M_z^2 \approx M_p^2 = (F')^2/(\mu_0\rho)$  in relation to the tokamak scaling  $B_p \approx 0.1B_z$  and  $v_p \approx 0.1v_z$ . In addition, to completely construct the equilibrium we have made the following choices

$$M_p^2 = C_p(u - u_b)^n(u_a - u)^m \quad (13)$$

$$C_p = M_{pa} \left[ \frac{m(u_a - u_b)}{m + n} \right]^{-m} \left[ \frac{n(u_a - u_b)}{m + n} \right]^{-n}$$

$$M_z^2 = C_z(u - u_b)^n(u_a - u)^m \quad (14)$$

$$C_z = M_{za} \left[ \frac{m(u_a - u_b)}{m + n} \right]^{-m} \left[ \frac{n(u_a - u_b)}{m + n} \right]^{-n}$$

$$B_z^2 = B_{z0}^2 \left[ 1 - \gamma \left( 1 - \frac{u}{u_b} \right) \right] \quad (15)$$

$$\rho = \rho_a \left( 1 - \frac{u}{u_b} \right)^\lambda \quad (16)$$

for the poloidal Mach function, axial Mach function, axial magnetic field and density, respectively, with  $B_{z0} = 2.24$  T,  $\rho_a = 4 \times 10^{-7}$  Kgr/m<sup>3</sup>,  $\gamma = 0.02$ ,  $u_a = 0$ ,  $u_b = 0.11$  W m<sup>2</sup>, (with the subscripts a and b indicating the magnetic axis and boundary respectively),  $\lambda = 0.5$ ,  $m = 9n$  and  $M_{za} = 1.1M_{pa}$  with various values of the parameters  $M_{pa}$  and  $n$ . Here, Eqs. (13) and (14) can describe Mach functions localized in the edge plasma region in connection with the L-H transition (in particular flows localized nearly in the one tenth of the exterior plasma will be considered as it is shown in Fig. 3); Eq. (15) represents a diamagnetic  $B_z(u)$  (Fig. 4). Then, (2) and (5) imply a pressure peaked on axis (Fig. 5).

Furthermore we have examined certain equilibrium characteristics by means of the safety factor, magnetic shear, axial current density, radial electric field and  $\mathbf{E} \times \mathbf{B}$  velocity shear, and found the following results.

1. The safety factor for both solutions shown in Figs. 6,7 is slightly affected by the flow. Also, the flow affects slightly the magnetic shear given by  $s(u) = 2(V/q)(dq/dV)$  as it can be seen in Fig. 8 for Equilibrium 1. A similar plot holds for Equilibrium 2.
2. The radial electric field for the two solutions has an extremum in the edge region which increases with flow (Figs. 9 and 10). The position of

the extremum, however, is nearly unaffected by the flow. These characteristics are indicative that the solutions may be relevant to the L-H transition as discussed in [23] where a similar behavior of the electric field was found (Fig. 3 therein).

3. The  $\mathbf{E} \times \mathbf{B}$  velocity shear which is believed to play a role in the transitions to improved confinement regimes of magnetically confined plasmas is given by

$$\omega_{E \times B} = \left| \frac{d}{dr} \left[ \frac{\mathbf{E} \times \mathbf{B}}{B^2} \right] \right| \quad (17)$$

where  $r$  is the length variable normal to the magnetic surfaces. For Equilibrium 1 it is plotted in Fig. 11; a similar plot holds for Equilibrium 2.  $\omega_{E \times B}$  is increased by the flow in the edge region outer from the local minimum while it remains nearly unaffected in the central region. This is another indication supporting the relevance of the solutions to the L-H transition.

4. The flow makes the axial (“toroidal”) current density profile hollow as shown in Fig. 12 for Equilibrium 1. (A similar  $j_{tor}$  profile is found for Equilibrium 2.) The larger the flow is the stronger the hollowness. Hollow  $j_{tor}$  profiles are usually related to the formation of internal transport barriers in tokamaks. However, despite of this characteristic and the fact that  $\omega_{E \times B}$  becomes maximum on the magnetic axis (Fig. 11) it is unlikely that the present equilibria are related to internal transport barriers because the safety factor is monotonically increasing from the magnetic axis to the plasma edge (Figs. 6, 7). According to observations in tokamaks, e.g [46] for JET and [47] for DIII-D, it is the reversed magnetic shear which plays a role in triggering the ITBs development. Also, as can be seen in Figs. 6 and 7 the flow makes the central  $q$ -values lower.

## 5 Stability consideration

We now consider the important issue of the stability of the solutions constructed in Section IV with respect to small linear MHD perturbations



by applying the sufficient condition of Ref. [44]. This condition states that a general steady state of a plasma of constant density and incompressible flow parallel to  $\mathbf{B}$  is linearly stable to small three-dimensional perturbations if the flow is sub-Alfvénic ( $M^2 < 1$ ) and  $A \geq 0$ , where  $A$  is given below by (18). Consequently, using henceforth dimensionless quantities we set  $\rho = 1$ . Also, for parallel flows ( $\mathbf{v} = M\mathbf{B}$ ) it holds  $M_p \equiv M_z \equiv M$ . In fact if the density is uniform at equilibrium it remains so at the perturbed state because of incompressibility [48]. In the  $u$ -space for axisymmetric equilibria  $A$  assumes the form

$$\begin{aligned}
A = & -\bar{g}^2 \left[ (\mathbf{j} \times \nabla u) \cdot (\mathbf{B} \cdot \nabla) \nabla u + \right. \\
& + \left. \left( \frac{M_p^2}{2} \right)' \frac{|\nabla u|^2}{(1 - M_p^2)^{3/2}} \left\{ \nabla u \cdot \nabla (B^2/2) + \right. \right. \\
& \left. \left. + \bar{g} \frac{|\nabla u|^2}{(1 - M_p^2)^{1/2}} \right\} \right] \quad (18)
\end{aligned}$$

with

$$\bar{g} := \frac{P'_s(u) - (M_p^2)' B^2/2}{1 - M_p^2}$$

Symbolic computation of  $A$  over a wide range of parametric values led to the following results:

1. Equilibrium 1 is not satisfied, since  $A < 0$  everywhere, while Equilibrium 2 is satisfied in an appreciable part of the plasma region. However, it is noted that since the stability condition is necessary,  $A < 0$  does not imply that an equilibrium is unstable. An example of the sign of  $A$  for Equilibrium 2 is given in the three-dimensional plot of Fig. 13. Also, profiles of  $A$  in the middle-plane  $y = 0$  for a static and a stationary equilibrium are shown in Fig. 14.
2. Increase of  $M_{pa}$  makes  $A$  more positive in the edge region as can be seen in the example of Fig. 14. A similar impact on  $A$  has the flow shear parameter  $n$  (Eq. (13)) as can be seen in Fig. 15 showing the profile of  $\delta A = A(y = 0, n = 2) - A(y = 0, n = 1)$ .
3. The equilibrium nonlinearity in connection with the parameters  $c_3$  and  $c_4$  has a stabilizing effect in the edge region as shown in the example of Fig. 16 plotting the profile of the difference  $\delta A$  between a nonlinear and a linear Equilibrium 2.

According to the above results and the believe that the sheared flow is developed during the L-H transition we conjecture that a static Equilibrium 1 could correspond to the L state and a stationary Equilibrium 2 with  $\mathbf{E} \times \mathbf{B} / B^2$  velocity shear to the H state. In a quasistatic evolution approximation the plasma could then evolve through successive states with increased sheared flow (increasing values of the parameters  $M_{pa}$  and  $M_{za}$  and most importantly increasing values of the shearing parameters  $m$  and  $n$ ).

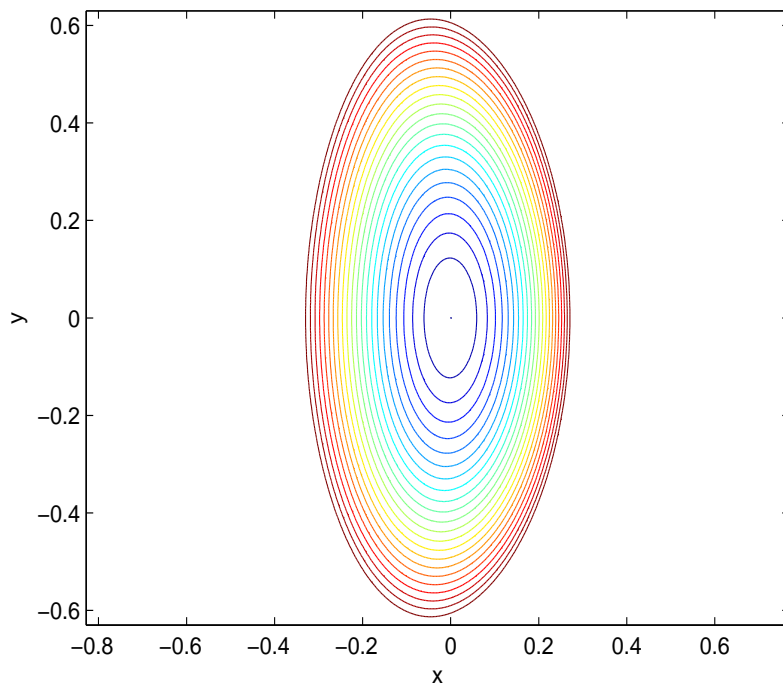


Figure 1: Equilibrium 1. The bounding flux surface corresponds to  $u_b = 0.11$ , with  $u_a = 0$ , for the magnetic axis. For this equilibrium the average value of  $|C_s|$  is 0.10.

## 6 Summary

Two classes of solutions of nonlinear two dimensional magnetohydrodynamic equilibria for bounded magnetically confined plasmas with sheared incom-

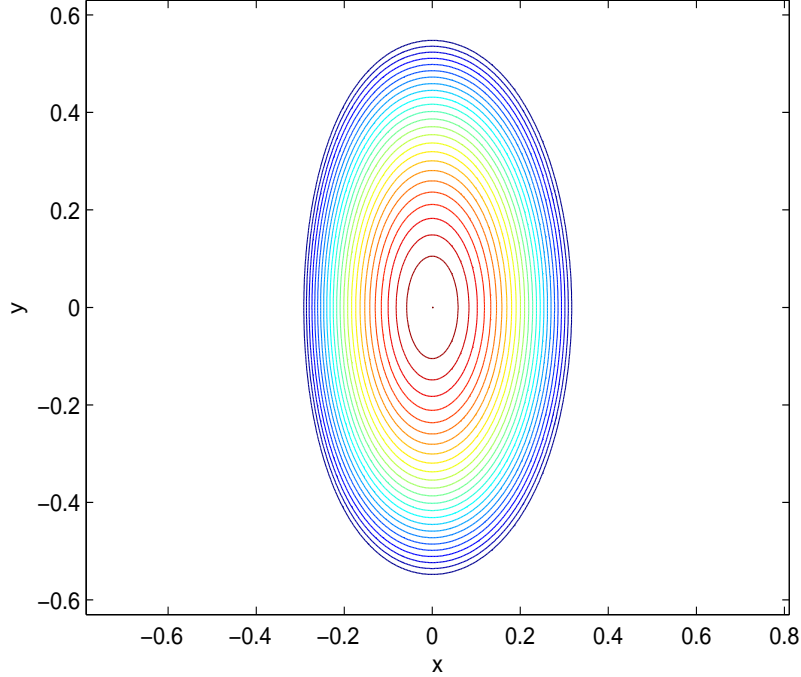


Figure 2: Equilibrium 2. The bounding flux surface corresponds to  $u_b = -0.05$ , with  $u_a = 0$ , for the magnetic axis. For this equilibrium the average value of  $|C_s|$  is 0.10.

pressible non parallel flows have been constructed in cylindrical ( $z$ -independent) geometry. The equilibria hold for four arbitrary surface functions which were chosen to be the plasma density, axial Mach function, poloidal Mach-function and static pressure.

After assigning the free functions, a systematic examination of equilibrium quantities and confinement figures of merit, as the safety factor, electric field and  $\mathbf{E} \times \mathbf{B}$  velocity shear for a variety of parametric values, implies that the equilibrium characteristics are qualitatively consistent with experimental evidence of the L-H transition. In addition, application of a sufficient condition for linear stability and parallel flow indicates that one stationary equilibrium being potential stable may describe the H-state and another static equilibrium not satisfying the stability condition the L-state. In addition the equilibrium non-linearity in conjunction with the flow and the flow shear

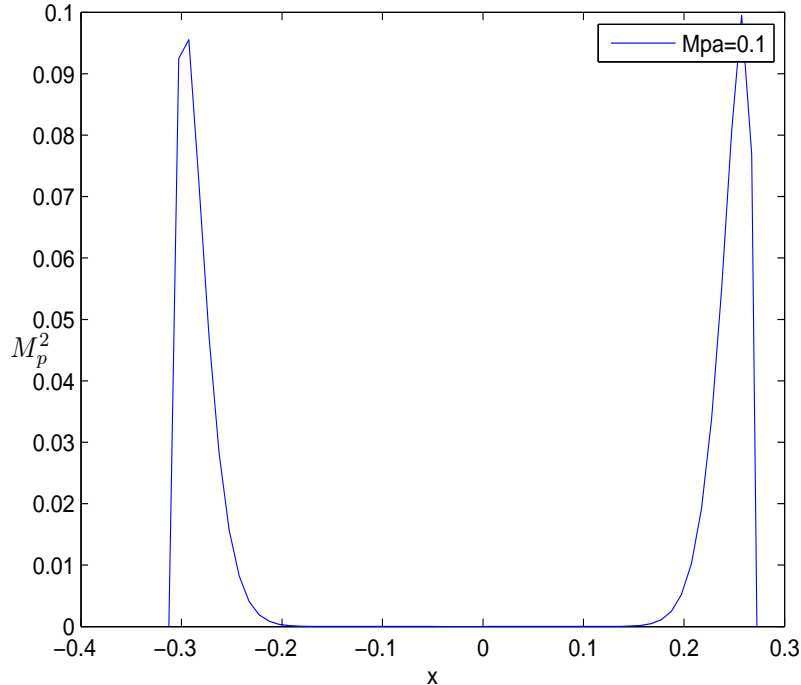


Figure 3: L-H transition-like Mach function in connection with Eq. (13) with  $n = 1$  and a maximum localized at a distance from the boundary as large as the on tenth of the minor radius.

may play a stabilizing role. Although understanding the physics of the L-H transition remains incomplete the results of the present study may shed some light towards that goal.

Finally it would be interesting trying to generalize these classes of solutions to up-down asymmetric configuration with a lower  $x$ - point in connection with the ITER project. Also the study could be extended to toroidal geometry in order to examine the impact of toroidicity.

## Acknowledgments

One of the authors (GNT) would like to thank Drs. Henri Tasso and

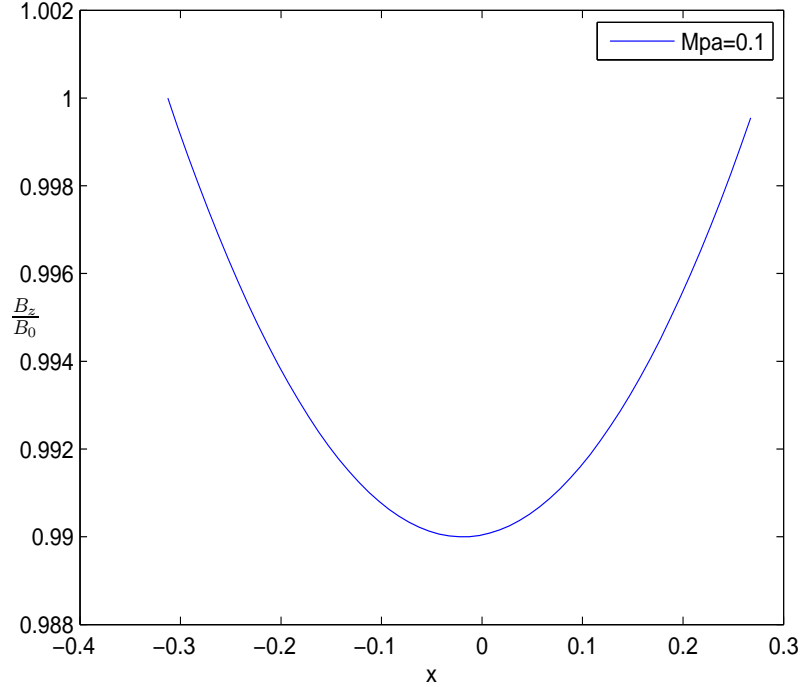


Figure 4: Typical diamagnetic axial magnetic field profile normalized with respect to the value at the magnetic axis in connection with Eq. (15) .

Calin Atanasiu for very useful discussions.

The work leading to this article was performed within the participation of the University of Ioannina in the Association Euratom-Hellenic Republic, which is supported in part by the European Union (Contract of Association No. ERB 5005 CT 99 0100) and by the General Secretariat of Research and Technology of Greece. The views and opinions expressed herein do not necessarily reflect those of the European Commission.

## References

- [1] V. D. Shafranov, Sov. Phys. JETP **6**, 545 (1958); Zh. Eksp. Teor. Fiz. **33**, 710 (1957).

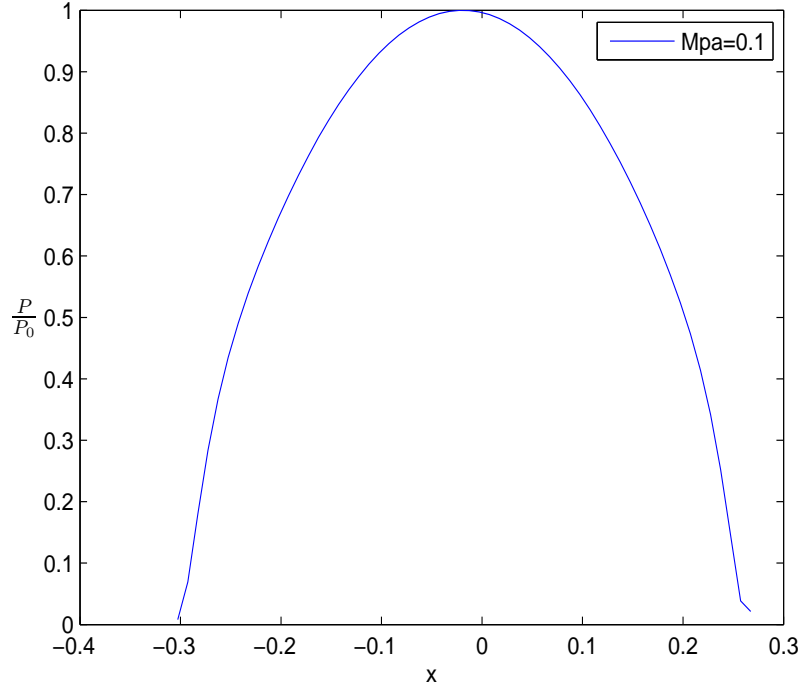


Figure 5: Pressure profile at  $y = 0$  for the Equilibrium 1.

- [2] H. Grad and H. Rubin, in *Proceedings of the Second United Nations Conference on the Peaceful Uses of Atomic Energy* (United Nations, Geneva, 1958), Vol. 21, p. 190.
- [3] L. S. Solovév, *Sov. Phys. JETP* **26**, 400 (1968); *Zh. Eksp. Teor. Fiz.* **53**, 626 (1976).
- [4] F. Herrnegger, in *Proceedings of the 5th European Conference on Controlled Fusion and Plasma Physics*, Grenoble, Vol. I, p. 26 (1972).
- [5] E. K. Maschke, *Plasma Phys.* **15**, 535 (1972).
- [6] H. L. Berk, J. H. Hammer, and H. Weitzner, *Phys. Fluids* **24**, 1758 (1981).
- [7] P. J. Mc Carthy, *Phys. Plasmas* **6**, 3554 (1999).

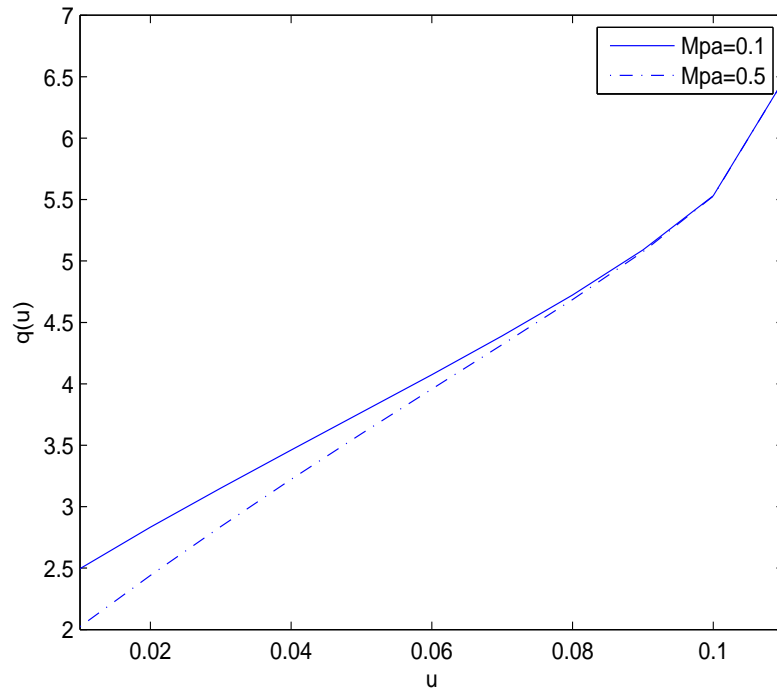


Figure 6: Safety factor for the solution of Equilibrium 1.

- [8] R. H. Weening, *Phys. Plasmas* **7**, 3654 (2000).
- [9] V. A. Yavorskij, K. Schoepf, Zh. N. Andrushchenko, B. H. Cho, V. Ya. Goloborod'ko and S. N. Reznik, *Plasma Phys. Controlled Fusion* **43**, 249 (2001).
- [10] C. V. Atanasiu, S. Gunter, K. Lackner and I. G. Miron *Phys. Plasmas* **11**, 3510 (2004).
- [11] A. J. Cerfon and J. P. Freidberg *Phys. Plasmas* **17**, 032502 (2010).
- [12] R. Srinivasan, L. L. Lao and M. S. Chu, *Plasma Phys. Control. Fusion* **52**, 035007 (2010).
- [13] S. Mukhopadhyay, *Bull. Am. Phys. Soc.* **45**, 364 (2000).
- [14] P. W. Terry, *Rev. Mod. Phys.* **72**, 109 (2000).

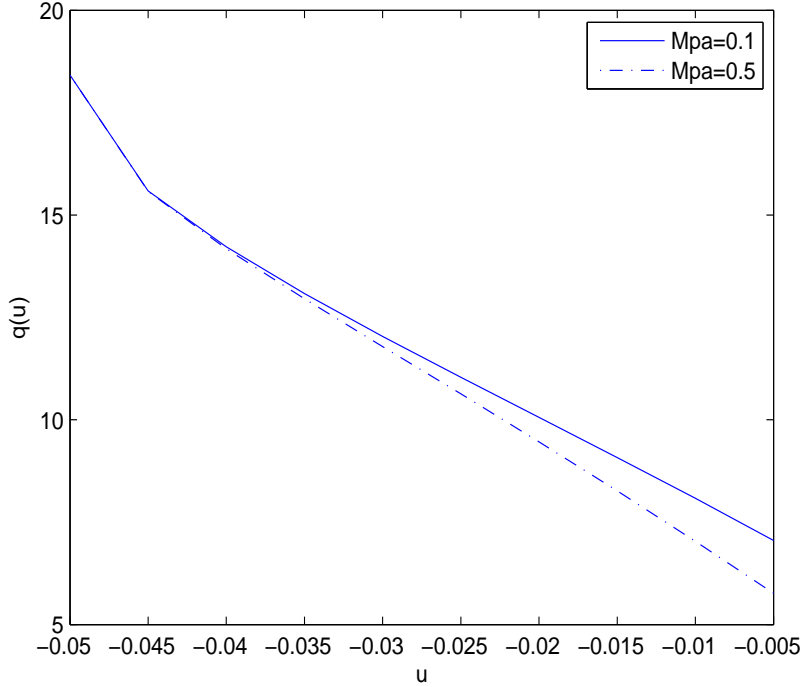


Figure 7: Safety factor for the solution of Equilibrium 2. Notice that the outer boundary surface corresponds to  $u = -0.05$  while the magnetic axis to  $u = -0.005$

- [15] E. K. Mashke and H. Perrin Phys. Lett. A **102**, 106 (1984).
- [16] R. A. Clemente and R. Farengo, Phys. Fluids **27**, 776 (1984).
- [17] J. M. Greene, Plasma Phys. Controlled Fusion **30**, 327 (1988).
- [18] G. N. Throumoulopoulos and G. Pantis, Plasma Phys. Controlled Fusion **38**, 1817 (1996).
- [19] G. N. Throumoulopoulos and H. Tasso, Phys. Plasmas **4**, 1492 (1997).
- [20] J. P. Goedbloed and A. Lifschitz, Phys. Plasmas **4**, 3544 (1997).
- [21] H. Tasso and G. N. Throumoulopoulos, Phys. Plasmas **5**, 2378 (1998).



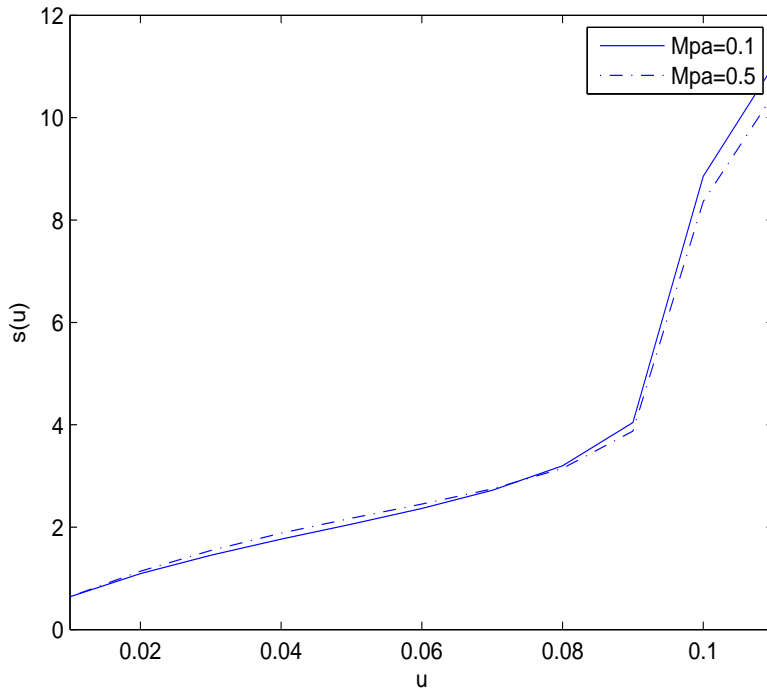


Figure 8: Magnetic Shear for the solution of Equilibrium 1. It is slightly affected by the presence of flow. A similar plot holds for Equilibrium 2.

- [22] R. Betti, J. P. Freidberg Phys. Plasmas **7**, 2439 (2000).
- [23] Ch. Simintzis, G. N. Throumoulopoulos G. Pantis and H. Tasso, Phys. Plasmas **8**, 2641 (2001).
- [24] S. I. Krasheninnikov, T. K. Soboleva and P. J. Catto, Phys. Lett. A **298**, 171 (2002).
- [25] G. Poulipoulis, G. N. Throumoulopoulos and H. Tasso, Phys. Plasmas **12**, 042112 (2005).
- [26] G. N. Throumoulopoulos, H. Weizner and H. Tasso, Phys. Plasmas **13**, 122501 (2006).

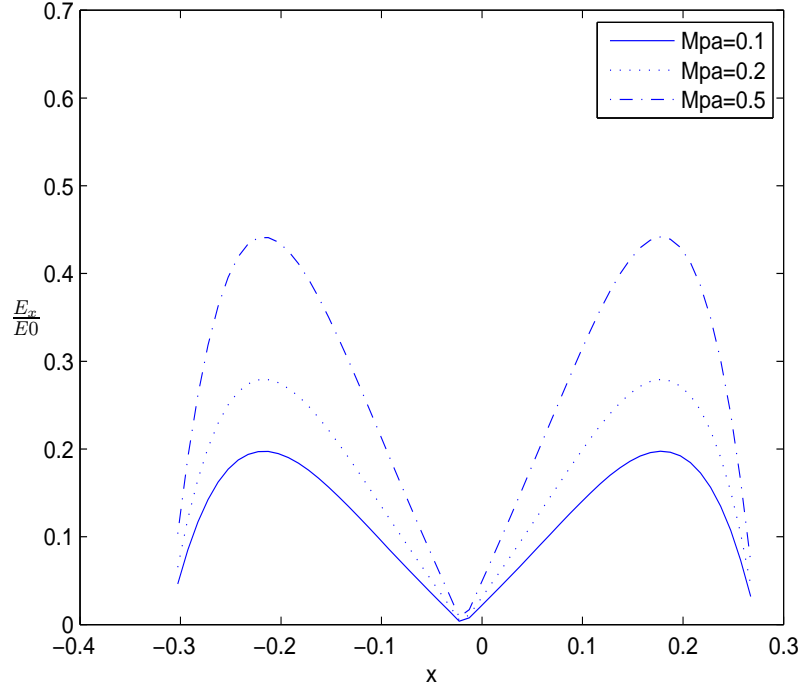


Figure 9: Normalized electric field with respect to  $E_0 = 280$  kV/m for the solution of Equilibrium 1. The extremum of the electric field increases with flow, the position of the extremum however is not significantly affected by it.

- [27] D. Apostolaki, G. N. Throumoulopoulos and H. Tasso, 35th EPS Conference on Plasma Phys. Hersonissos, 9-13 June 2008 ECA Vol. **32**, P-2.057 (2008).
- [28] G. N. Throumoulopoulos, H. Tasso, G. Poulipoulis, J. Plasma Physics **74**, 327 (2008)
- [29] A. H. Khater and S. M. Moawad, Phys. Plasmas **16**, 122506 (2009).
- [30] Ap Kuiroukidis, Plasma Phys. Control. Fusion **52**, 015002 (2010).
- [31] Ap Kuiroukidis and G. N. Throumoulopoulos, Plasma Phys. Control. Fusion **53**, 125005 (2011).

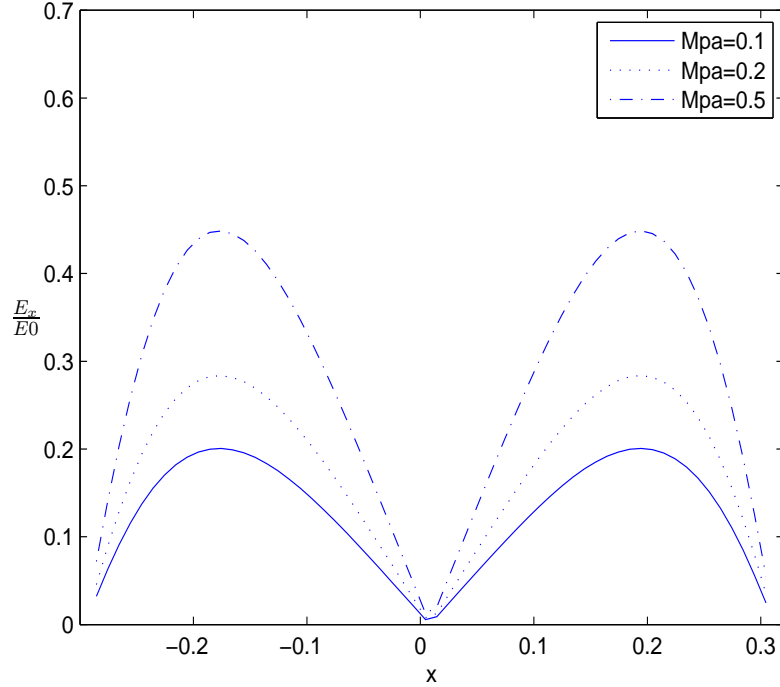


Figure 10: Electric field for the solution of Equilibrium 2. The extremum of the electric field increases with flow, the position of the extremum however is not significantly affected by it.

- [32] K. H. Tsui, C. E. Navia, A. Serbeto and H. Shigueoka, *Phys. Plasmas* **18**, 072502 (2011).
- [33] Bingren Shi, *Nucl. Fusion* **51**, 023004 (2011).
- [34] G. N. Throumoulopoulos, H. Tasso, *Phys. Plasmas* **19**, 014504 (2012).
- [35] Ap Kuiroukidis and G. N. Throumoulopoulos, *Phys. Plasmas* **19**, 022508 (2012).
- [36] G. N. Throumoulopoulos, H. Tasso and G. Poulipoulis, *J. Phys. A: Math. Theor.* **42**, 335501 (2009).
- [37] G. N. Throumoulopoulos and H. Tasso *Phys. Plasmas* **17**, 032508 (2010).

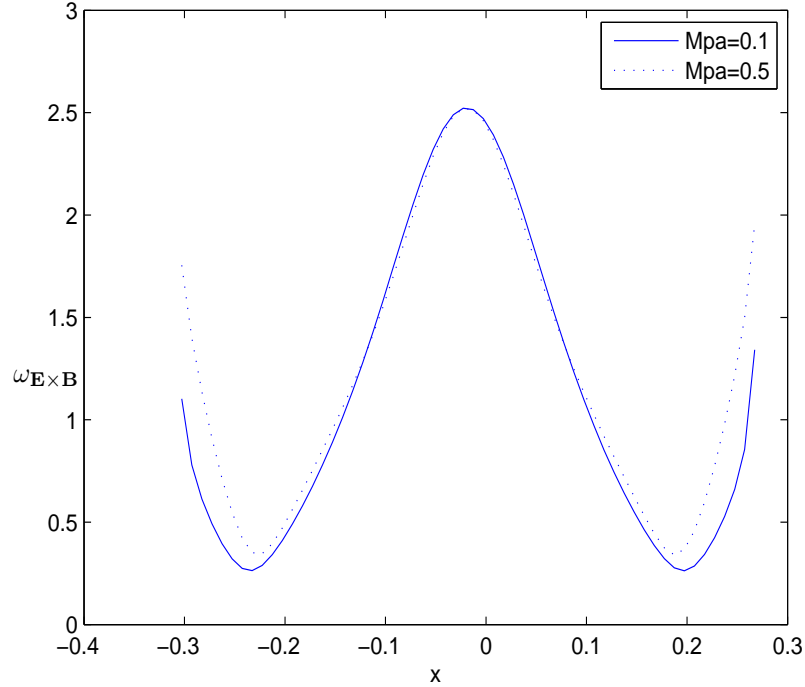


Figure 11: The  $\mathbf{E} \times \mathbf{B}$  velocity shear, for the solution of Equilibrium 1. It increases slightly with the presence of flow in the edge region. Similar plot holds for Equilibrium 2.

- [38] E. R. Solano, Plasma Phys. Control. Fusion **46**, L7 (2004).
- [39] V. I. Ilgisonis and Yu. I. Pozdnyakov, Plasma Physics Reports, **30**, 988 (2004).
- [40] J. Garcia and G. Giruzzi, PRL **104**, 2050003 (2010).
- [41] K. H. Tsui and C. E. Navia Phys. Plasmas **19**, 012505 (2012)
- [42] S. Friedlander, M. M. Vishik, Chaos **5**, 416 (1995).
- [43] V. A. Vladimirov and K. I. Ilin, Phys. Plasmas **5**, 4199 (1998).
- [44] G. N. Throumoulopoulos and H. Tasso Phys. Plasmas **14**, 122104 (2007).

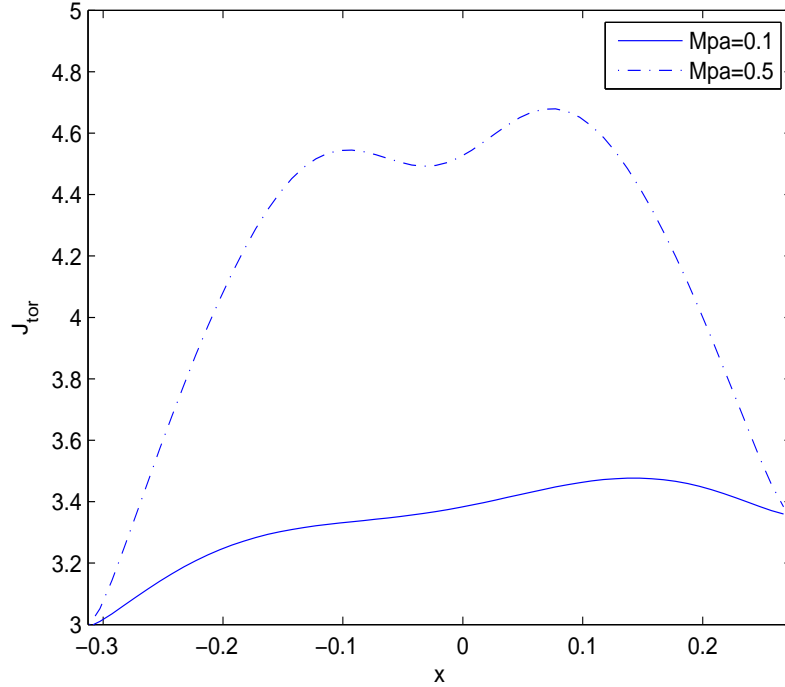


Figure 12: Axial current density in MA as a function of the flow parameter  $M_{pa}$ , for the solution of Equilibrium 1. As the flow increases a hollow profile in the core of the equilibrium appears and it becomes larger for larger values of the flow.

- [45] W. Malfliet, J. Comp. Appl. Math **164-165**, 529 (2004).
- [46] P. C. de Vries, E. Joffrin, M. Brix C. D. Challis, K. Cromb e, B. Esposito et al., Nucl. Fusion **49**, 075007 (2009).
- [47] M. W. Shafer, G. R. McKee, M. E. Austin K. H. Burrell, R. J. Fonck, and D. J. Schlossberg, Phys. Rev. Lett. **103**, 075004 (2009).
- [48] H. Tasso and G. N. Throumoulopoulos, J. Plasma Physics **78**, 1 2012.

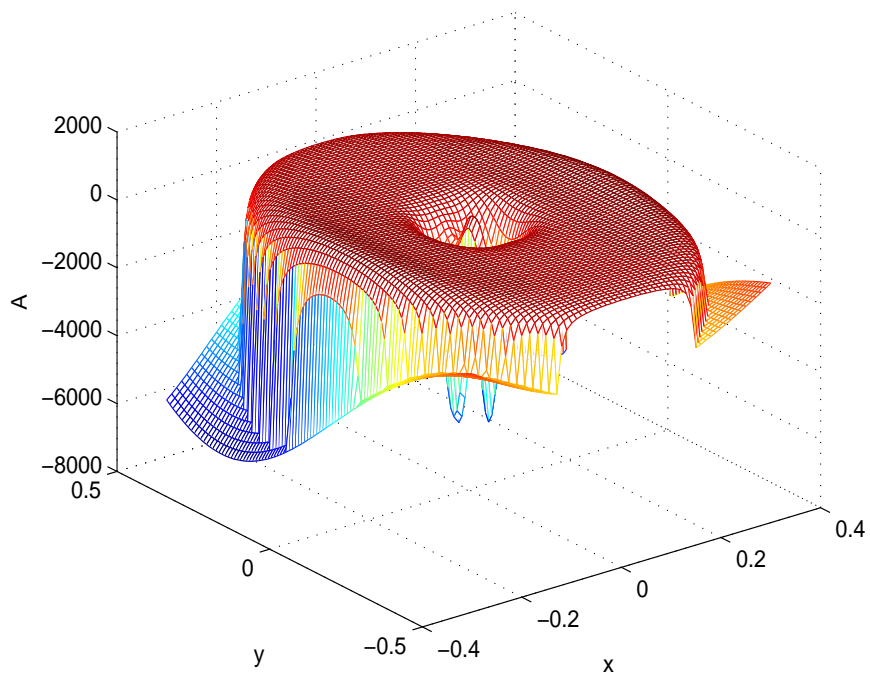


Figure 13: Stability function for the solution of Equilibrium 2. For most part of the equilibrium is positive and assumes negative values only in the core of the equilibrium.

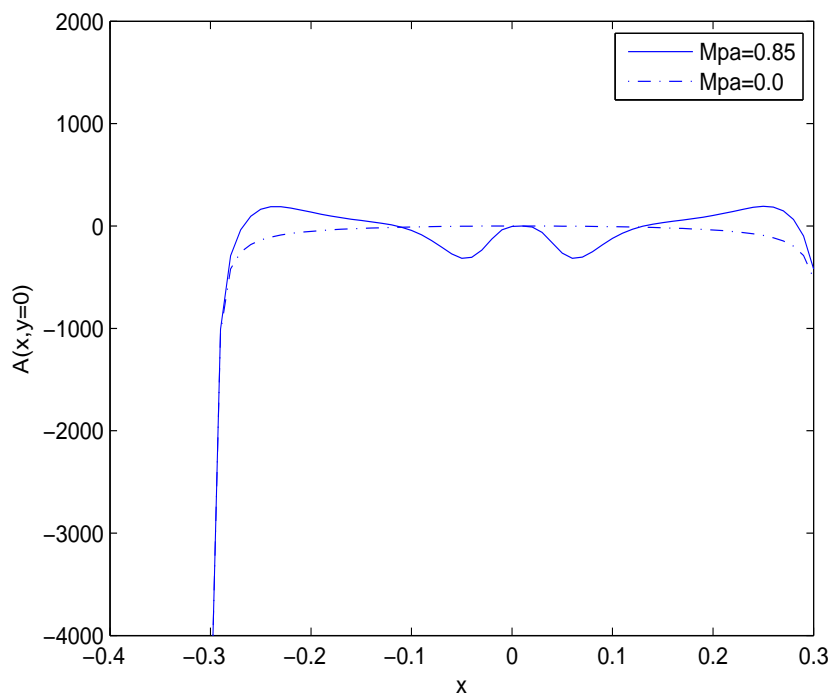


Figure 14: Plot of the stability function  $A$ , at  $y=0$ , for the second equilibrium for nonzero values of the nonlinearity parameters  $c_3=-3.099$ ,  $c_4=1.033$ . Increasing the flow parameter  $M_{pa}$  appears to improve stability for most part on the middle-plane except for the center of the equilibrium

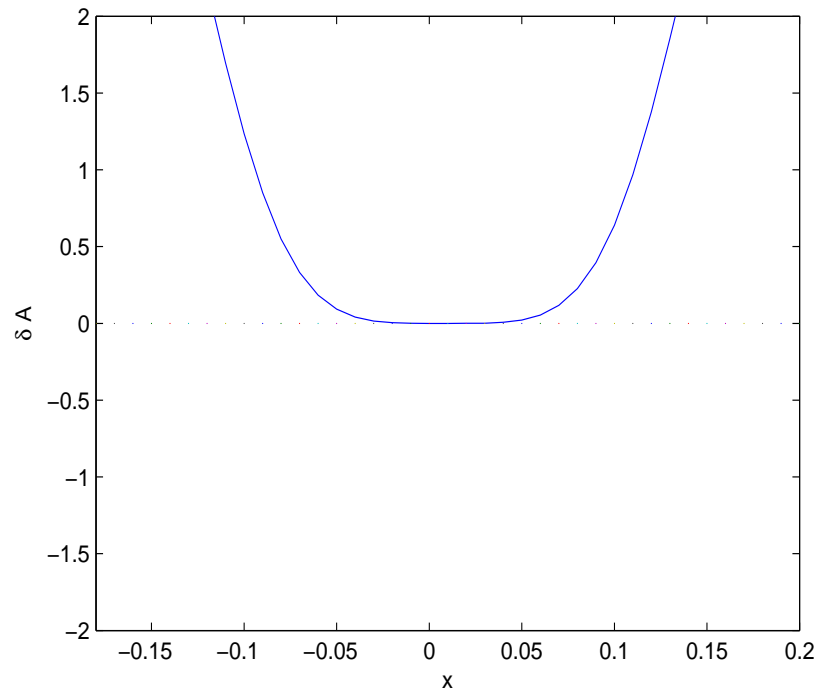


Figure 15: Plot of the difference  $\delta A = A(n = \dots) - A(n = \dots)$  for  $c3 = -3.099$ ,  $c4 = 1.033$  and  $Mpa = 0.1$  clearly indicating that the stability is improved ( $\delta A > 0$ ) at the external part of the middle-plane  $y = 0$  as the flow-shear parameter  $n$  increases. The dotted line represents the  $x$ -axis.



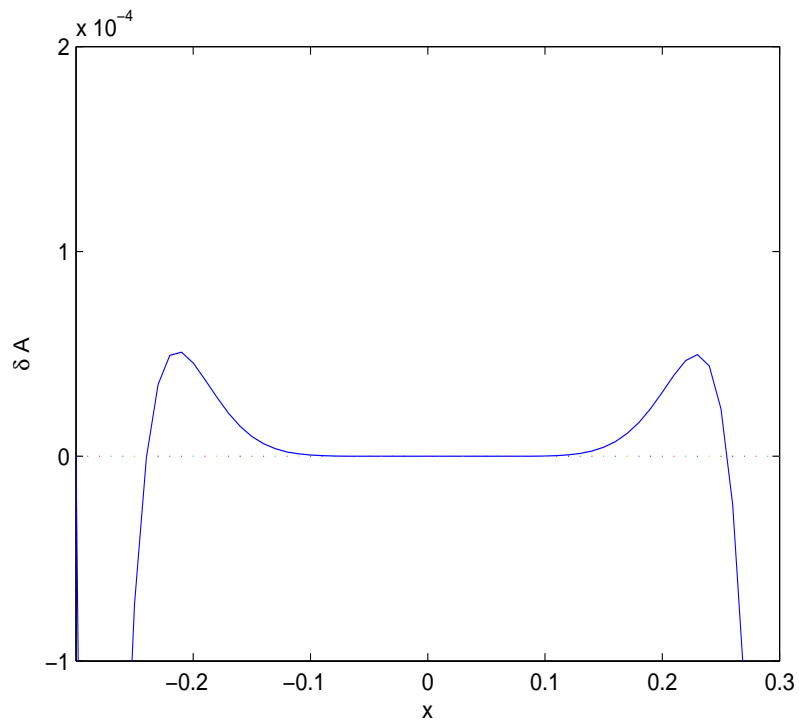


Figure 16: Plot of the profile  $\delta A = A(c_3 = -3.099, c_4 = 1.033) - A(c_3 = c_4 = 0)$  at  $y = 0$  indicating that the nonlinearity has a stabilizing effect ( $\delta A > 0$ ) in the edge region

